Electronic Supporting Information (ESI)

1. Materials and Instrumentations

All general reagents and solvents were purchased from Sinopharm Chemical Reagent Co., L td, Energy Chemical and Tokyo Chemical Industry. 1,2-bis(4-bromophenyl)-1,2-diphenylethene (2Br-TPE) was synthesized by following a previously reported method with some modifications. The synthetic details of 2Br-TPE were provided in Supporting Information. ^{1}H NMR and ^{13}C NMR spectra were recorded on a Varian Unity 600 MHz and 150 MHz spectrometer. Mass spectra were recorded on an Agilent 6210 TOF-MS spectrometer using electrospray ionization. The infrared spectra were recorded on a Shimadzu IR Prestige-21 FT-IR Spectrometer with pressed KBr pellets. UV-vis absorption spectra were recorded on PerkinElmer Lambda 750. X-ray crystal structures were obtained by using Bruker D8 CMOS detectors. The powder XRD patterns were recorded on a Bruker D8 ADVANCE X-ray diffractometer. Data were collected from 5°–50° 2θ, with the operating power set to 40 kV/40 mA. Thermogravimetric analyses (TGA) were performed under nitrogen in the temperature range 25–650 °C with a heating rate of 10 °C min^{-1} on a GA-500 instrument. Solid fluorescence quantum yields were measured using a Hamamatsu absolute PL quantum yield spectrometer C11347 Quantaurus-QY. Fluorescence lifetimes were determined with a Hamamatsu C11367-11 Quantaurus-Tau time-resolved spectrometer. Theory calculations were performed using the density functional theory (DFT) with the B3LYP hybrid functional.

2. Synthesis

2Br-TPE. Synthesis of the ligand 1,2-bis(4-bromophenyl)-1,2-diphenylethene (2Br-TPE) began with the reaction of solid (4-bromophenyl)(phenyl)methanone (5 g, 19.2 mmol) and Znic (2.48 g, 38.4 mmol) with $TiCl_4$ (20 mL, 20 mmol) in THF (50 mL) at -5 °C, and then heated to 75 °C for 6 h under nitrogen to produce 1,2-bis(4-bromophenyl)-1,2-diphenylethene (2Br-TPE), which was purified via silica gel column chromatography in ~75% yield.[1,2] ^{1}H NMR (600 M Hz, $CDCl_3$), δ (TMS, ppm): 7.19–7.13 (m, 4H), 7.07–7.02 (m, 6H), 6.93–6.89 (m, 4H), 6.84–6.77 (m, 4H).^{13}C NMR ($CDCl_3$, 150 MHz), δ (TMS, ppm): 141.84, 141.30, 139.25, 131.85, 130.14, 129.87, 126.99, 126.79, 125.96. ESI (FAB): m/z = 490.2 $[M + H]^+$.

3. Additional Data

Table S1. Crystal data and structure refinements for complex **1**.

Compound	complex **1**
Formula	$C_{28}H_{18}O_{4.33}Zn_{1.33}$
M	510.92
crystal system	rhombohedral
space group	*R*
a/Å	28.1564(14)
b/Å	28.1564(14)
c/Å	32.140(3)
α/deg	90.00
β/deg	90.00
γ/deg	120.00
V/Å^3	22067(3)
Z	18
temperature/K	293(2)
λ(radiation wavelength)/Å	0.71073
D(g/cm^3)	0.692
reflections collected	31202
$R1^a$[I >2σ(I)]	0.0592
$wR2^b$[I >2σ(I)]	0.1330
goodness-of-fit	1.033
CCDC no.	1588480

[a] $R1 = \sum |F_o - F_c| / \sum |F_o|$. [b] $wR2 = [\sum [w(F_o^2 - F_c^2)^2] / w(F_o^2)^2]^{1/2}$

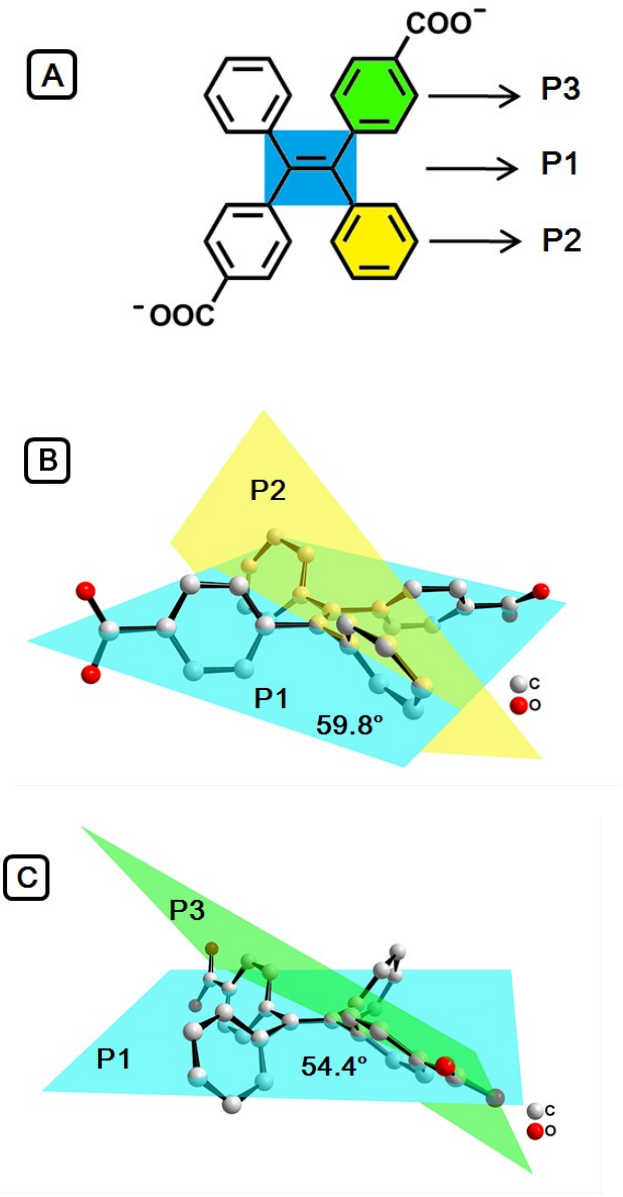

Fig. S1 (A) The plane of the two C atoms forming central C=C double bond and four C atoms surround them is named P1. The planes of free phenyl ring adjacent to C=C bond are named P2. The planes of phenyl ring connected with carboxylic group are named P3. The average dihedral angles are labeled for (B) P1-P2 and (C) P1-P3 in complex **1**.

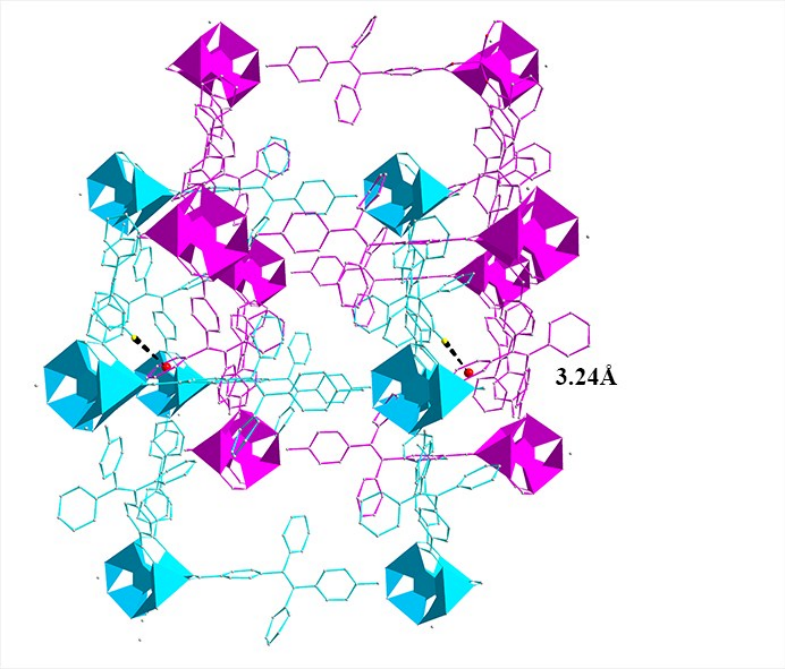

Fig. S2 C–H···π interactions of complex **1** (the black dotted lines are labeled for C–H···π interactions).

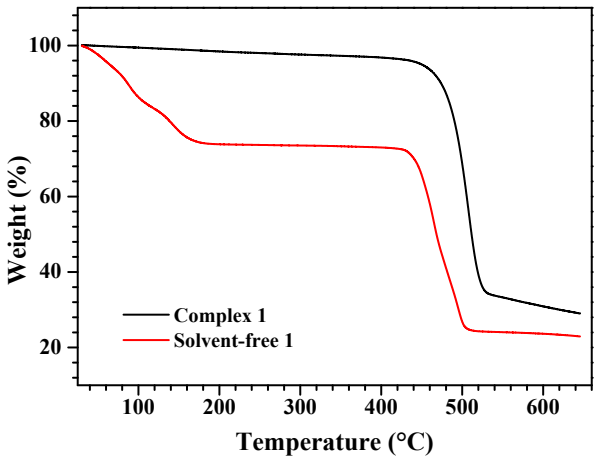

Fig. S3 Thermogravimetric (TG) analyses of complex **1** and solvent-free **1**.

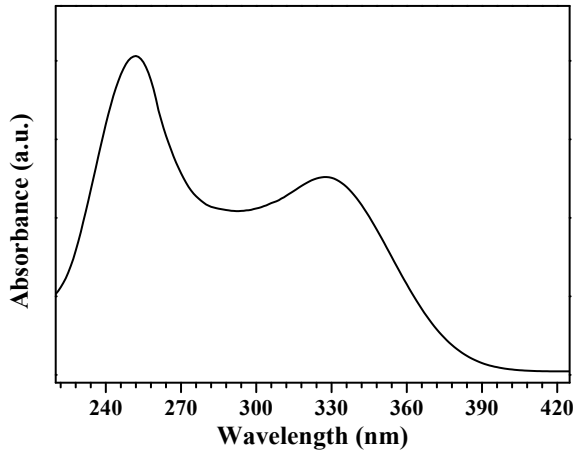

Fig. S4 UV-vis absorption spectrum of H_2BCTPE in THF solution.

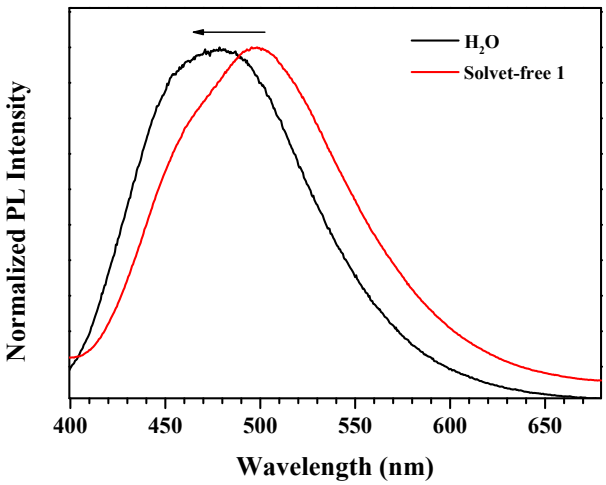

Fig. S5 Emission spectra of solvent-free **1** dispersed in H_2O (λ_{ex}= 365 nm).

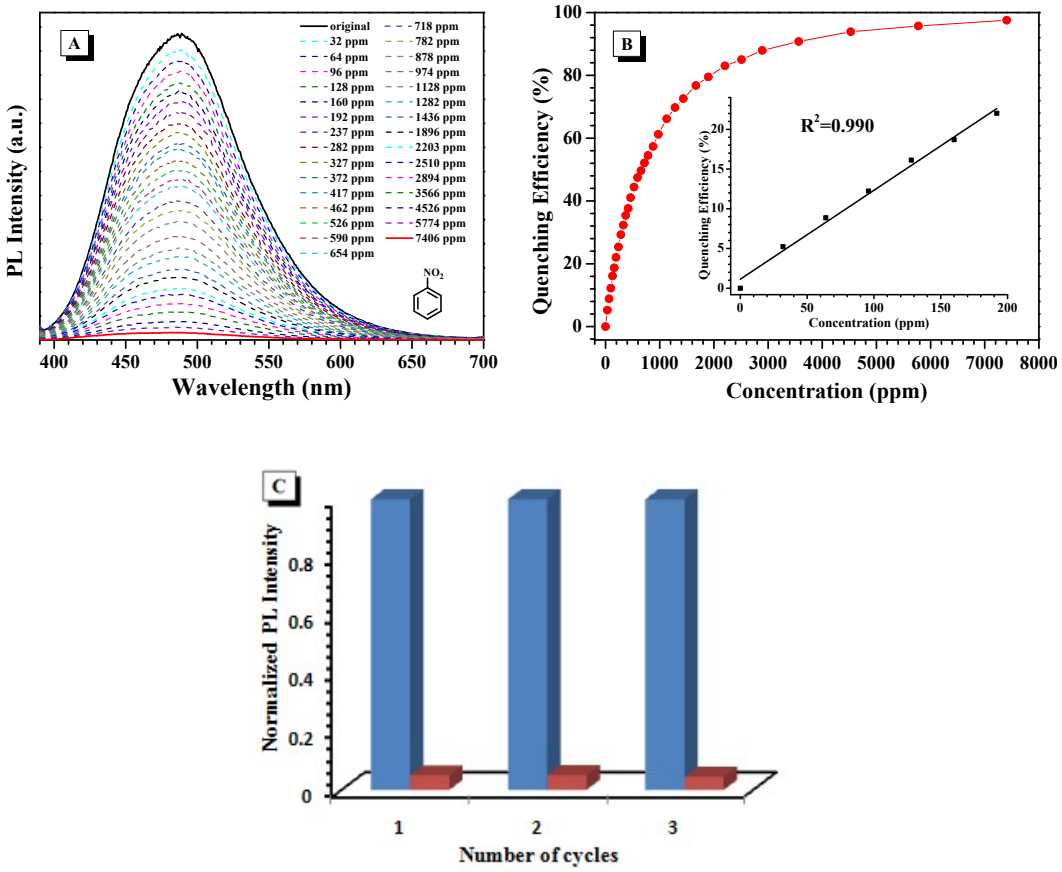

Fig. S6 (A) Fluorescence titration of solvent-free **1** suspension with varied concentrations of nitrobenzene (λ_{ex}= 365 nm). (B) Correlation between the quenching efficiency and concentration of nitrobenzene. Inset: the linear relationship of fitting (0–200 ppm). (C) Reproducibility of the quenching ability of solvent-free **1** with nitrobenzene. (The blue bars represent the initial fluorescence intensity, and the red bars represent the intensity upon addition of 7000 ppm.)

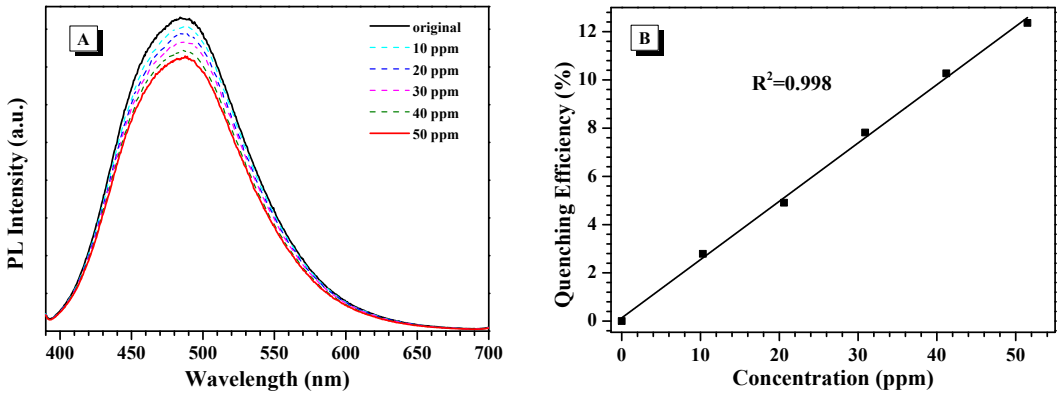

Fig. S7 (A) Low-concentration fluorescence titration of nitrobenzene. (B) The fitting relationship for low-concentration fluorescence titration of solvent-free **1** with nitrobenzene.

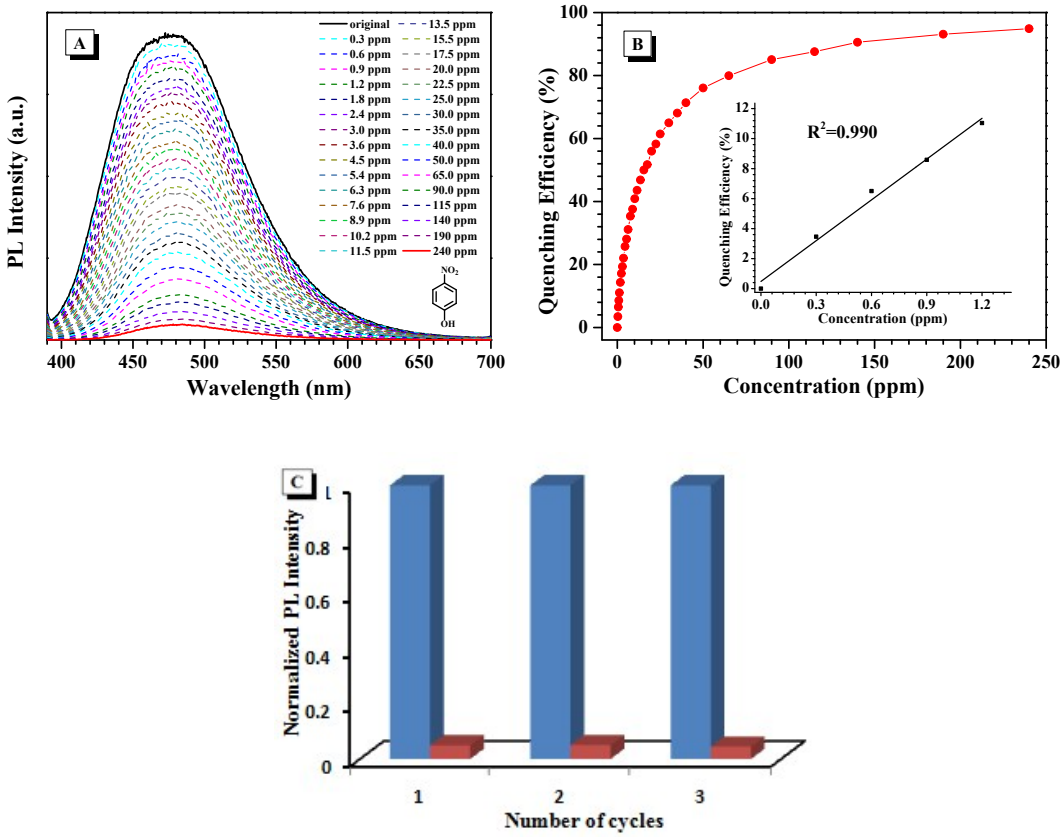

Fig. S8 (A) Fluorescence titration of solvent-free **1** suspension with varied concentrations of 4-nitrophenol (λ_{ex}= 365 nm). (B) Correlation between the quenching efficiency and concentration of 4-nitrophenol. Inset: the linear relationship of fitting (0–1.2 ppm). (C) Reproducibility of the quenching ability of solvent-free **1** with 4-nitrophenol. (The blue bars represent the initial fluorescence intensity, and the red bars represent the intensity upon addition of 240 ppm.)

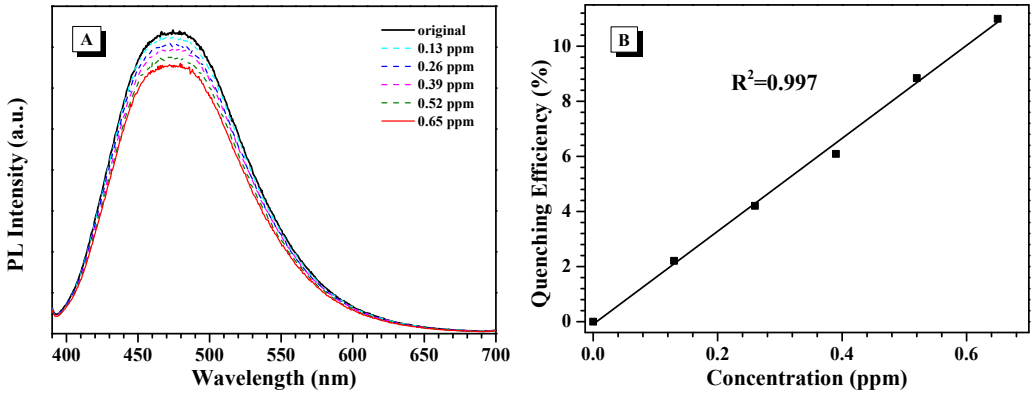

Fig. S9 (A) Low-concentration fluorescence titration of 4-nitrophenol. (B) The fitting relationship for low-concentration fluorescence titration of solvent-free **1** with 4-nitrophenol.

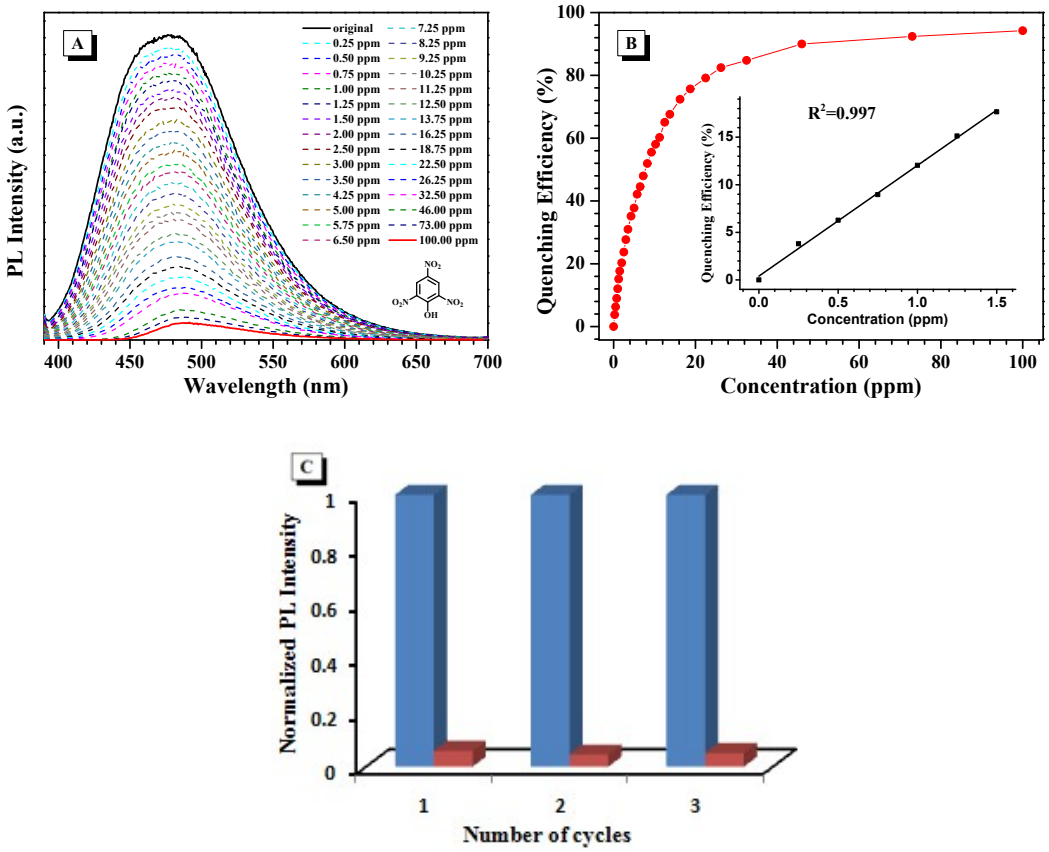

Fig. S10 (A) Fluorescence titration of solvent-free **1** suspension with varied concentrations of 2,4,6-trinitrophenol (λ_{ex}= 365 nm). (B) Correlation between the quenching efficiency and concentration of picric acid. Inset: the linear relationship of fitting (0–1.5 ppm). (C) Reproducibility of the quenching ability of solvent-free **1** with 2,4,6-trinitrophenol. (The blue bars represent the initial fluorescence intensity, and the red bars represent the intensity upon addition of 100 ppm.)

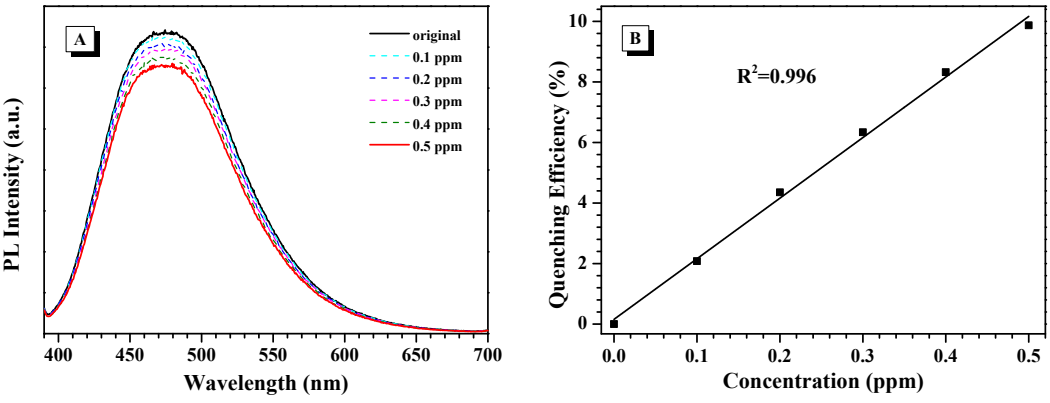

Fig. S11 (A) Low-concentration fluorescence titration of 2,4,6-trinitrophenol. (B) The fitting relationship for low-concentration fluorescence titration of solvent-free **1** with 2,4,6-trinitrophenol.

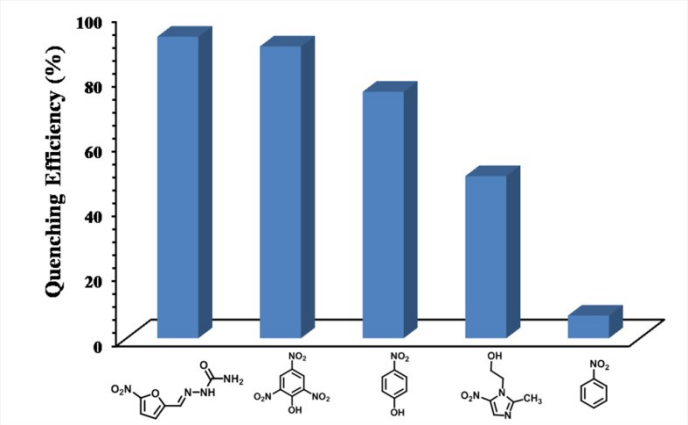

Fig. S12 The quenching efficiencies of solvent-free **1** suspension by 50 ppm different analytes (λ_{ex}= 365 nm).

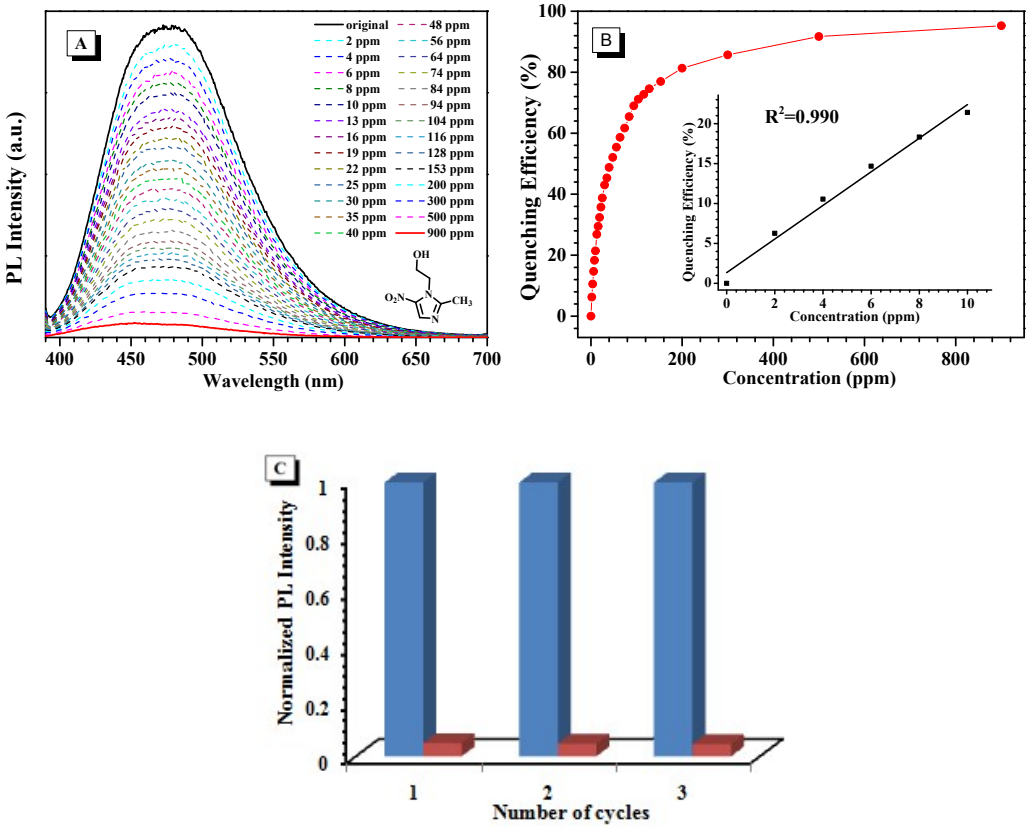

Fig. S13 (A) Fluorescence titration of solvent-free **1** suspension with varied concentrations of metronidazole (λ_{ex}= 365 nm). (B) Correlation between the quenching efficiency and concentration of picric acid. Inset: the linear relationship of fitting (0–10 ppm). (C) Reproducibility of the quenching ability of solvent-free **1** with metronidazole. (The blue bars represent the initial fluorescence intensity, and the red bars represent the intensity upon addition of 900 ppm.)

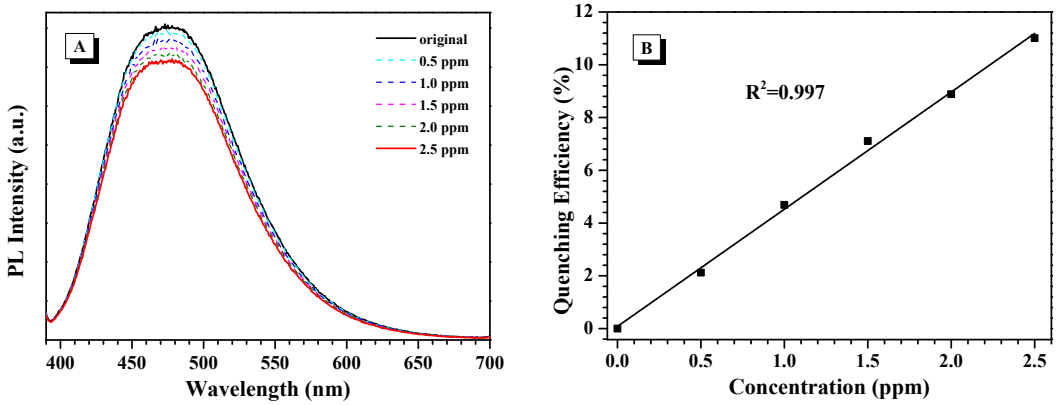

Fig. S14 (A) Low-concentration fluorescence titration of metronidazole. (B) The fitting relationship for low-concentration fluorescence titration of solvent-free **1** with metronidazole.

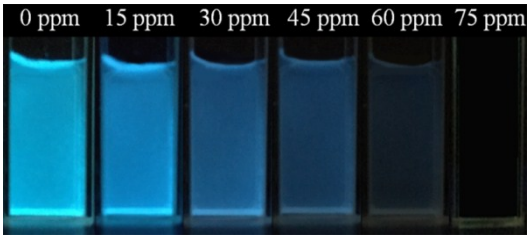

Fig. S15 Fluorescence photos of solvent-free **1** suspension with gradually increased nitrofurazone.

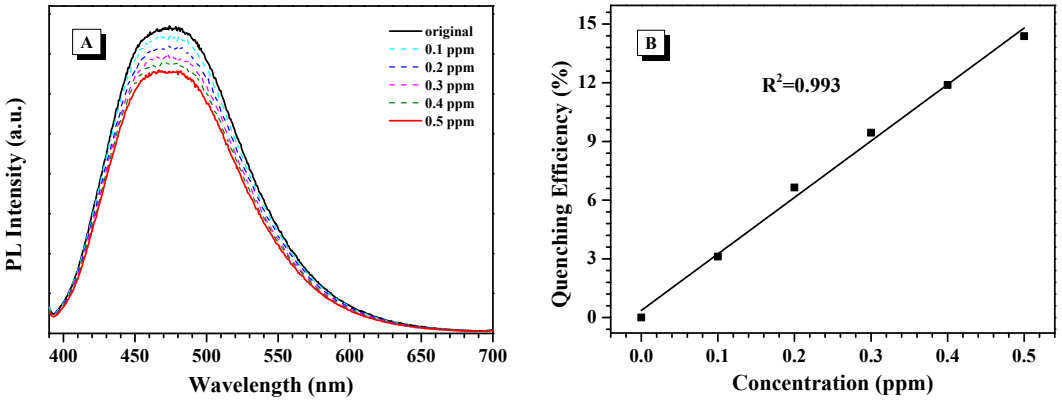

Fig. S16 (A) Low-concentration fluorescence titration of nitrofurazone. (B) The fitting relationship for low-concentration fluorescence titration of solvent-free **1** with nitrofurazone.

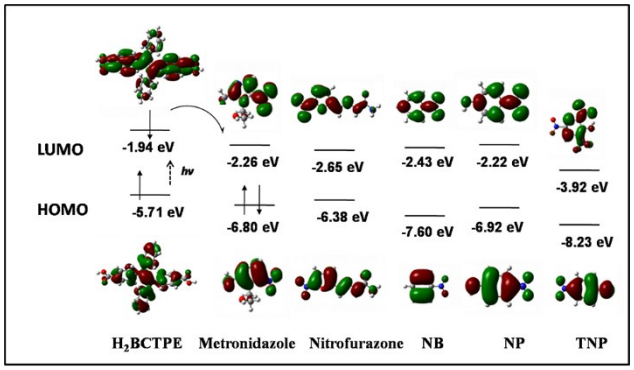

Fig. S17 The HOMO and LUMO energy levels of H_2BCTPE in complex **1**, metronidazole, nitrofurazone, NB, NP and TNP.

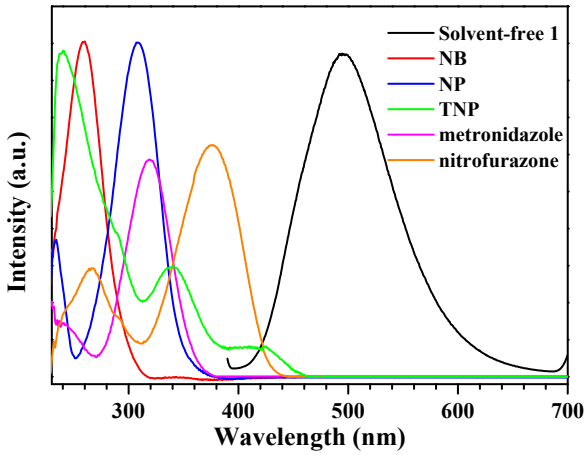

Fig. S18 The absorption spectra of nitro-containing analytes and the emission spectrum of solvent-free **1**.

4. Reference

1. Y. Ma, H. Ma, Z. Yang, J. Ma, Y. Su, W. Li and Z. Lei, *Langmuir*, 2015, **31**, 4916.
2. G. Lin, H. Peng, L. Chen, H. Nie, W. Luo, Y. Li, S. Chen, R. Hu, A. Qin, Z. Zhao and B. Z. Tang, *ACS Appl. Mater. Interfaces*, 2016, **8**, 16799.